some organs such as the heart lack the microsomal ethanol-oxidizing system (*7*) yet are targets of alcohol-induced damage. Although acetaldehyde is highly reactive and could damage hepatocytes, its concentration in blood may be markedly overestimated (*11, 23*). Indeed, liver-produced acetaldehyde has not been demonstrated to directly injure organs that lack endogenous production of this aldehyde. Finally, the genetic components of the selectivity of organ damage induced by ethanol (*2, 12, 13*) and the development of alcohol-induced heart muscle disease in the absence of pancreatitis or cirrhosis (*10*) cannot be attributed to acetaldehyde in blood because each of the organs is exposed to similar concentrations of circulating acetaldehyde derived from the liver (*11*). Thus there must be gene products residing in such organs that ultimately produce or modulate tissue injury and are responsible for the selectivity of organ damage.

These considerations suggest that other biochemical mediators are involved in alcohol-induced organ injury. Our results indicate that a nonoxidative pathway for ethanol metabolism exists in the human organs that are commonly injured by alcohol abuse but lack oxidative ethanol metabolism. Thus fatty acid ethyl esters could be such mediators involved in the production of alcohol-dependent syndromes. In organs that lack oxidative pathways, organ specificity of ethanol-induced injury may be related to rates of fatty acid ethyl ester synthesis and degradation. Of course, interaction between the oxidative and nonoxidative pathways may occur.

A potential mechanism of injury by fatty acid ethyl esters was recently demonstrated in isolated mitochondria (*24*). The fatty acid ethyl esters, acting as a shuttle for fatty acid between cellular fatty acid binding sites and the mitochondria, bind to these organelles where they are hydrolyzed and release free fatty acids, known uncouplers of oxidative phosphorylation. Impaired mitochondrial function has been well established in alcoholic cardiomyopathy, and the release of free fatty acids has been proposed as one of the initial events leading to alcohol-induced pancreatitis (*25*) as well as alcohol-induced heart disease (*26*). Since the amount of fatty acid ethyl ester formed in a parenchymal target organ (Fig. 3) is linearly related to blood alcohol concentrations, individuals who ingest large amounts of alcohol will synthesize more fatty acid ethyl esters.

In summary, nonoxidative ethanol metabolism occurs in humans in the organs most commonly injured by alcohol abuse. Since some of these organs lack oxidative ethanol metabolism and because acetaldehyde cannot be the sole chemical mediator producing selective damage, fatty acid ethyl esters and their metabolism may have a role in the production of alcohol-induced injury. Thus fatty acid ethyl esters as well as acetaldehyde or other as yet unidentified chemical agents may serve as a link between alcohol intake and development of alcohol-induced disease.

REFERENCES AND NOTES

1. L. J. West, *Ann. Intern. Med.* 100, 405 (1984).
2. C. R. Cloninger, *J. Psychiatric Treat. Eval.* 5, 487 (1983).
3. S. B. Thacker, R. L. Veech, A. A. Vernon, D. D. Rutstein, *Alcohol. Clin. Exp. Res.* 8, 375 (1984).
4. T.-K. Li, *ibid.* 5, 451 (1981).
5. S. Harada, D. P. Agarwal, H. W. Goedde, *Adv. Exp. Med. Biol.* 132, 31 (1980).
6. B. L. Vallee and T. J. Bazzone, *Curr. Top. Biol. Med. Res.* 8, 219 (1983).
7. C. S. Lieber and L. M. DeCarli, *Science* 162, 917 (1968).
8. A. Lochner, R. Cowley, A. J. Brink, *Am. Heart J.* 78, 770 (1969).
9. H. J. Raskin and L. J. Sokoloff, *J. Neurochem.* 19, 273 (1972).
10. J. H. Lefkowitch and J. J. Fenoglio, *Hum. Pathol.* 14, 457 (1983).
11. C. J. P. Eriksson and H. W. Sippel, *Biochem. Pharmacol.* 26, 241 (1979).
12. Editorial, *Lancet* 1985-I, 1427 (1985).
13. A. Hrubec and G. S. Omenn, *Alcohol. Clin. Exp. Res.* 5, 207 (1981).
14. P. M. Kinnunen and L. G. Lange, *Anal. Biochem.* 140, 567 (1984).
15. L. G. Lange, *Proc. Natl. Acad. Sci. U.S.A.* 79, 3954 (1982).
16. S. Mogelson and L. G. Lange, *Biochemistry* 23, 4075 (1984).
17. J. J. Barboriak, D. P. Barboriak, A. J. Anderson, R. G. Hoffman, *Curr. Alcohol.* 8, 293 (1981).
18. J. H. Chin, J. H. Goldstein, D. B. Goldstein, *Mol. Pharmacol.* 13, 435 (1977).
19. T.-K. Li, W. F. Bosron, W. P. Dafeldecker, L. G. Lange, B. L. Vallee, *Proc. Natl. Acad. Sci. U.S.A.* 74, 4378 (1977).
20. A. Harada, S. Misawa, D. P. Agarwal, H. W. Goedde, *Am. J. Hum. Genet.* 32, 8 (1980).
21. T.-K. Li, *Adv. Enzymol.* 45, 427 (1977).
22. G. D. Wendell and R. G. Thurman, *Biochem. Pharmacol.* 28, 273 (1972).
23. H. U. Nuuntinen, M. P. Slaspuro, M. Valle, K. O. Lindross, *Eur. J. Clin. Invest.* 14, 306 (1984).
24. L. G. Lange and B. E. Sobel, *J. Clin. Invest.* 72, 724 (1983).
25. P. Saharia, S. Margolis, G. D. Zuideman, J. L. Cameron, *Surgery* 82, 60 (1977).
26. O. M. Pachinger, H. Tillmanns, J. C. Mao, J. M. Fauvel, R. J. Bing, *J. Clin. Invest.* 52, 2690 (1973).

27. Supported in part by NIH grant HL-30152.

5 June 1985; accepted 18 November 1985

Optical Image Quality and the Cone Mosaic

ALLAN W. SNYDER, TERRY R. J. BOSSOMAIER, AUSTIN HUGHES

Contrary to the orthodox view that optical image quality should "match" the photoreceptor grain, anatomical data from the eyes of various animals suggest that the image quality is significantly superior to the potential resolution of the cone mosaic in most retinal regions. A new theory is presented to explain the existence of this relation and to better appreciate eye design. It predicts that photoreceptors are potentially visible through the natural optics.

THE IDEA THAT THE PHOTORECEPTOR mosaic should "match" the optical image quality is well entrenched in the vison literature. It is implicitly assumed that the optical image quality is fixed and that a photoreceptor grain evolved to best encode it. Using comparative biological data, we now show that this classical belief is wrong. In fact, the data are consistent with the opposite view, that the retinal grain is set by biological needs and that it is the optics that molds itself to best serve the retina. This simple biological explanation has major new implications for understanding the design of photopic eyes, particularly those with highly differentiated retinal topography such as visual streaks. It predicts correctly that optical image quality should be significantly superior to the photoreceptor grain and, in animals with nonuniform retinas, be adaptively modulated away from the optic axis rather than passively deteriorating due to classical aberrations.

Few biological data are available, but it appears that cone undersampling is widespread, if not the general rule. Several examples are shown in Table 1, which gives the sampling bandwidth or highest spatial frequency ν_s that can be unambiguously reconstructed by the cone mosaic; the optical bandwidth or maximum spatial frequency ν_o passed by the optics in bright light (smallest pupil diameter); the sampling efficiency ν_s/ν_o, which specifies the amount of undersampling; the posterior nodal distance of the eye P; and the ratio d/d_c, where d is the cone diameter and d_c the distance between cone centers (*1*). Matched sampling occurs when the anatomical resolving power equals the optical resolving power ($\nu_s = \nu_o$), or, equivalently (*2*), when the half-height width $\Delta\rho$

A. W. Snyder, Institute of Advanced Studies, Australian National University, Canberra, 2600, and National Vision Research Institute, Melbourne, 3053 Australia.
T. R. J. Bossomaier, Institute of Advanced Studies, Australian National University, Canberra, 2600.
A. Hughes, National Vision Research Institute, Melbourne, 3053 Australia, and Institute of Advanced Studies, Australian National University, Canberra, 2600.

Table 1. Examples of measurements of P, d/d_c, ν_s, ν_o, and ν_s/ν_o for man, cat, rat, and garter snake, taken from the literature (*16, 18–25*).

Animal (eccentricity)	P (mm)	d/d_c (μm)	ν_s (cycle/deg)	ν_o (cycle/deg)	ν_s/ν_o
Man (0°)	17	0.85 to 0.9	55 to 60	65 to 70	0.79 to 0.92
Man (10°)	17	0.4 to 0.6	13	20 to 60	0.22 to 0.65
Cat (0°)	12.5	0.28	20	30	0.66
Rat (0°)	3.33	0.13	2.1	4.6	0.46
Snake (0°)	2.5	0.85 to 0.9	2.15	4.5 to 7.2	0.30 to 0.48

of the point spread function (3) obeys $\Delta\rho \simeq \Delta\phi\sqrt{3}$, $\Delta\phi$ is the distance between cone centers for a hexagonal lattice. Thus, an Airy disk (diameter, $\sim 2\Delta\rho$) covers an area of about ten cones in an all-cone retinal region. Undersampling occurs when $\nu_o > \nu_s$, that is, a sampling efficiency of 30 percent with $3\nu_s = \nu_o$ corresponds to an Airy disk slightly smaller than an individual cone inner segment in an all-cone retina.

These examples suggest that optical image quality in vertebrate eyes is significantly superior to the cone mosaic in at least some portion of the retina, as in most compound eyes (*4*). We propose that the cone mosaic is set by biological needs while optical image quality is the comparatively flexible component in the visual chain. Thus, we ask what optical image quality best serves a given cone mosaic. In engineering terminology this is equivalent to adjusting the signal to match a given detector, which is the inverse of the normally posed problem.

If the visual system were noise-free, then the optical image quality should match the cone resolving power ($\nu_o = \nu_s$) because exact image reconstruction is possible, in theory, for all spatial frequencies ($\nu < \nu_s$) potentially resolved by the cone matrix. Because of noise, however, there is only a finite contrast sensitivity at each frequency so that exact image reconstruction is not possible. Furthermore, natural light is incoherent so that the optical modulation transfer function approaches zero as ν approaches ν_s. Thus with matched optics there is a significant loss in high spatial frequency detail because these frequencies are more vulnerable to noise contamination. There is clearly a significant gain in image contrast at the level of the cone output by improving the optical image quality beyond matched conditions, because the optical modulation transfer function is then flatter over all frequencies that can be resolved by the cone matrix.

We argue that local cone density has a definite functional role, otherwise fewer cones would be required (*5*). Biological needs set the animal's subjective resolution. Thus the image quality must at least be sufficient for threshold detection (*6*) of a grating at the anatomical sampling frequency ν_s. This criterion sets the minimum undersampling ν_s/ν_o possible for a given cone mosaic (dashed curve in Fig. 1). Additional improvement in image quality comes at the expense of image distortion, known as aliasing, which may manifest itself as "blind" spots when the image of a point is confined to rod regions between cones (*7*). We use information theory to assess the trade-off between gain in contrast sensitivity and the penalty of aliasing for a given pupil size and cone mosaic (*8*). The optimum amount of undersampling ν_s/ν_o in an eye then depends on the properties of natural scenes—the brightest patches and highest contrasts normally encountered are about 10^4 cd/m^2 and 30 percent, respectively (*1, 9*)—and on the spatial correlation, which tests the limiting spatial performance of a given cone mosaic (*10*). This leads to the unbroken curve in Fig. 1, and, apart from the human fovea, gives a reasonable fit to the biological data in Table 1. Our results assume an achromatic retina and an integration time set by the cones. However, the human fovea is dichromatic, with the capacity for a protracted fixation time. Optimizing the optics for either of these capabilities allows for only a small amount of undersampling, in agreement with the biological data (*11*).

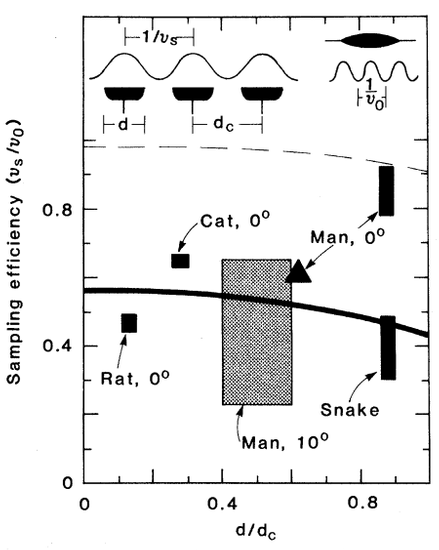

Fig. 1. Theoretical optimum sampling efficiency (unbroken curve) derived from information theory (*17*) compared with the biological data in Table 1. The figure assumes that cone inner segments are equal in diameter, that is, small values of d/d_c result from a high rod and cone density. The dashed curve (*6*) gives the minimum optical image quality to detect a grating of frequency ν_s.

The garter snake provides the most direct test of the theory in an all-cone retinal region. First, it is an all-cone retina of nearly uniform density, so that the same considerations apply equally at all retinal positions. More important, the snake pupil is about half the diameter of man's pupil in bright light, yet image quality is only about one-tenth as good (*12*). In other words, there is no pressure for diffraction-limited optics in this snake. Nevertheless, the optical image quality is about three times better than that required to match the cone mosaic. This strategy is consistent with the theory presented here.

The fact that visual photoreceptors undersample the optical image (*13*) may seem surprising, because electronic communication devices are often designed to oversample (*14, 15*). The conventional engineering approach, when applied to the design of animal eyes, attempts to obtain the minimum density of photoreceptors that will encode all images on the retina for a specified image quality and error tolerance. The solution is then to employ matched sampling. However, in real eyes the cone mosaic is known to vary across the retina according to the habitat and life-style of the animal (*16*). Thus the biologically relevant question asks what optical image quality distribution best serves the specified cone mosaic. The solution is to vary optical image quality across the retina in harmony with, but everywhere superior to, the cone mosaic. This suggests that photoreceptors are potentially visible through the natural optics of the eye, and this has now been demonstrated in two instances (*12*).

REFERENCES AND NOTES

1. For a hexagonal array, $\nu_s \simeq 1.0\ P/d_c$ [A. W. Snyder and W. H. Miller, *J. Opt. Soc. Am.* **67**, 696 (1977); A. W. Snyder, in *Handbook of Sensory Physiology*, H. Autrum, Ed. (Springer, New York, 1977), vol. 7, part 6A, pp. 225–314; *J. Comp. Physiol.* **116**, 161 (1977)].
2. We use $\nu_s = 1/(3)^{1/2}\Delta\phi$, where $\Delta\phi$ is the angle between cone centers measured in object space, assuming hexagonal packing (*1*). ν_o approximately equals $1/\Delta\rho$, where $\Delta\rho$ is the width at half-height of the point spread function. Thus $\nu_s/\nu_o = \Delta\rho/\Delta\phi\sqrt{3}$. For diffraction-limited optics $\Delta\rho \simeq \lambda/D$, where D is the pupil diameter and λ the wavelength in vacuum.
3. The point spread is the image due to a small luminous object.
4. R. Wehner, in *Handbook of Sensory Physiology*, H. Autrum, Ed. (Springer, New York, 1977), vol. 7, part 6C, pp. 297–311.
5. This role need not necessarily be for resolution; it could be for the detection and location of moving objects.
6. Threshold grating detection depends on the signal-

to-noise ratio of the cones which at maximum equals that set by photon noise, that is, $CM\sqrt{N}$, where M is the modulation transfer function of the optics, C is the grating contrast, and N is the mean number of photons absorbed by each cone (*1*). N is proportional to luminance, the cone inner segment area, and $(1/F_{number})^2$. This leads (*1*) to an expression for the minimum possible undersampling given approximately by $\nu_s/\nu_o \simeq [k - 0.13 \ (d/d_c)^2]^{1/2}$, where $k = (\ln C\sqrt{N})/3.56$. We have approximated the point spread function by a Gaussian (*1*), that is, the angular width $\Delta\rho$ of the point spread function at the cone output is related to the cone inner segment diameter $\Delta\rho_r$ and the half-width diameter of the optical spread function $\Delta\rho_{o_2}$ both in angular terms, such that $\Delta\rho^2 = \Delta\rho_r^2 + \Delta\rho^2_o$. $N \simeq 10^4$ photons in bright light for man, rats, and cats, but for snakes, $N \simeq 10^5$, assuming, in all cases, an integration time of 30 m/sec and a maximum luminance of 10^4 cd/m^2. The discrepancy between N for snakes and N for the other animals is greatly exaggerated here because we have neglected the huge Stiles-Crawford effect due to the wide inner segments of snake cones. Furthermore, undersampling is advantageous in the presence of a significant Stiles-Crawford effect because this effect raises the signal-to-noise level of the optical image at intermediate frequencies (at the expense of higher frequencies). The maximum contrast normally encountered in nature is ~0.25.

7. If certain retinal regions are devoted exclusively to detecting and locating moving objects, aliasing distortion may be of minor concern. It is possible to have nearly 50 percent undersampling without suffering any aliasing distortion at the level of ganglion cells. This requires having more cones than ganglion cells, with the retina wired so that ganglion cells can only detect frequencies below their anatomical sampling frequency ν_g, where the cone sampling frequency obeys $2\nu_s = \nu_o + \nu_g$. Thus, the cones can undersample by an amount $2(\nu_s/\nu_o) = 1 + \nu_g/\nu_o$ with an alias-free signal at the ganglion cell level. The cat eye (Table 1) is consistent with this strategy because $\nu_o \simeq 30$ cycles per degree (cpd), $\nu_s \simeq 20$ cpd, and $\nu_g \simeq 10$ cpd. The information within the spatial frequency band ν_g to ν_s need not be discarded but can be used in parallel for detection and location of moving objects.
8. Information theory determines the total number of different scenes an eye can distinguish [A. W. Snyder, S. B. Laughlin, D. G. Stavenga, *Vision Res.* **17**, 1163 (1977)]. We subtract from this total the number of scenes produced by frequencies above and then find the image quality that maximizes this difference (*17*).
9. S. B. Laughlin, *Z. Naturforsch. Teil C* **36**, 910 (1981).
10. The spatial correlation of the object world depends on the distribution and size of objects that reflect the majority of light and has an approximately exponential falloff for naturally occurring scenes (*9*). We argue that the cone grain has a definite functional role (*1*) or there would be fewer cones. Thus, to determine the approximate optical image quality, we choose a class of natural scenes that tests the limiting performance of spatial vision for a given cone matrix. Such scenes can be characterized by a correlation function about equal to the cone spacing, or, more precisely, the width at half-height equals the center-to-center cone separation. Most naturally occurring scenes of interest to an animal are considerably more correlated than this and thus have less high-frequency energy. However, it is only those natural scenes of interest which are comparatively uncorrelated that limit the amount of undersampling, since they suffer aliasing distortion. In other words, if the above assumptions are prejudiced, it is against too much undersampling, so that the unbroken curve in Fig. 1 may be slightly lower. This leads to the same expression for ν_s/ν_o as in (*6*), but with $k = 0.32$, or reduced by about 0.58 from detection theory (*17*).
11. The greater the signal-to-noise ratio across the cones, the less undersampling is desirable. The signal-to-noise ratio is increased by extending the neural integration time and by removing correlation between neurons by having dissimilar spectral cone types (*17*).
12. M. Land and A. W. Snyder [*Vision Res.* **25**, 1519 (1985)] measured an optical modulation transfer function of 35 percent at the anatomical resolution frequency ν_s. W. S. Jagger (*ibid.*, p. 729) demonstrates that oversampling does not occur in the cane toad eye and that adjacent receptors are resolvable through the natural optics.
13. In the developing kitten eye, optical and retinal organization varies so as to preserve optimal sampling over a twofold change in eye size (A. Hughes and R. O. L. Wong, in preparation) and a range of improving image quality. The adult retinal organization is discussed by A. Hughes [*Exp. Brain Res.* **42**, 196 (1981); in *Progress in Retinal Research*, N. N. Osborne and G. J. Chader, Eds. (Pergamon, Oxford, 1985), vol. 4, pp. 243–313].
14. A. B. Carlson, *Communication Systems* (McGraw-Hill, New York, 1968).
15. According to J. I. Yellot, Jr. [*Science* **221**, 382 (1983); *Vision Res.***22**, 1205 (1982); *ibid.* **24**, 281 (1984)], cone undersampling is the unavoidable consequence of "fixed optical components" preventing image quality from being matched over a nonuniform retina. There is no known theoretical constraint supporting this contention [A. Hughes, in *Visual Neuroscience*, J. Pettigrew, K. Sanderson, W. R. Levick, Eds. (Cambridge Univ. Press, Cambridge, in press), chap. 5]. The snake eye, with its uniform cone mosaic, is an exception to his claim. He further postulated that cones "assume an optimally irregular arrangement that avoids Moiré distortion of high frequency and minimizes sampling noise for low frequencies," but this has been disputed [A. S. French, A. W. Snyder, D. G. Stavenga, *Biol. Cybern.* **27**, 229 (1977); J. Hirsch and R. Hylton, *Vision Res.* **24**, 347 (1984); T. R. J. Bossomaier, A. W. Snyder, A. Hughes, *ibid.* **25**, 145 (1985)].
16. A. Hughes, in *Handbook of Sensory Physiology*, F. Crescitelli, Ed. (Springer, New York, 1977), vol. 7, part 5, pp. 613–756.
17. T. R. J. Bossomaier and A. W. Snyder, in preparation.
18. G. Westheimer, in *Handbook of Sensory Physiology*, D. Jameson and L. M. Hurvich, Eds. (Springer, New York, 1977), vol. 2, part 4, pp. 170–187.
19. W. H. Miller, *ibid.*, vol. 7, part 6A, H. Autrum, Ed. (Springer, New York, 1977), pp. 69–143.
20. F. W. Campbell and R. W. Gubisch, *J. Physiol. (London)* **186**, 558 (1966).
21. G. Østerberg, *Acta Ophthalmol. Suppl.* **6**, 1 (1935).
22. J. A. M. Jennings and W. N. Charman, *Vision Res.* **21**, 445 (1981).
23. R. H. Steinberg, M. Reid, P. L. Lacy, *J. Comp. Neurol.* **148**, 229 (1973).
24. J. G. Robson and C. Enroth-Cugell, *Vision Res.* **18**, 159 (1978).
25. W. Krause, *Int. Monatsh. Anat. Physiol.* **12**, 46 (1895).
26. We thank W. S. Jagger for confirming earlier measurements of P for the garter snake (Table 1). G. Westheimer suggested using information theory to determine the optimum sampling efficiency.

2 May 1985; accepted 13 September 1985

Technical Comments

The Sympathochromaffin System and the Pituitary-Adrenocortical Response to Hypoglycemia

Mezey *et al.* (*1*) reported that, in rats, the β-adrenergic antagonist propranolol blocked the plasma ACTH response to insulin injection, and they suggested that insulin stimulates ACTH release by a mechanism in which catecholamines of peripheral origin act directly on the anterior pituitary. Their finding that direct application of insulin to pituitary cells in vitro did not evoke ACTH release is consistent with in vivo evidence that the counterregulatory responses, including sympathochromaffin activation and cortisol secretion, which follow insulin injection are the result of decrements in plasma glucose, not of insulin itself (*2*). There is, however, substantial evidence that peripheral catecholamines do not play a critical role in the pituitary-adrenocortical response to plasma glucose decrements in humans. First, administration of propranolol, with or without the α-adrenergic antagonist phentolamine, did not reduce the plasma cortisol response to insulin-induced hypoglycemia (*3*), to the late decrement in plasma glucose that follows glucose ingestion (*4*), or to the decrement in plasma glucose that results from suppression of glucagon secretion in the postabsorptive state (*5*) in humans. Second, patients with diabetes who had deficient epinephrine secretory responses to plasma glucose decrements exhibited plasma cortisol increments during hypoglycemia that were similar to those of patients with normal epinephrine responses (*6*). Third, normal increments in plasma cortisol in response to intravenously administered 2-deoxy-D-glucose, which is thought to produce cellular glucopenia, occurred in patients with cervical spinal cord transections and no sympathochromaffin response (*7*). Fourth, elevations of epinephrine (*8*) or of norepinephrine (*9*) to plasma concentrations that spanned their respective physiologic ranges did not stimulate cortisol secretion in normal humans. Although none of the human studies cited assessed ACTH secretion as such, stimulation of cortisol secretion is a direct function of the plasma ACTH level and is the only action of ACTH of established biologic importance. Thus, the suggestion of Mezey *et al.* from their studies in rats does not appear to apply to humans.

PHILIP E. CRYER
Metabolism Division, Washington University School of Medicine, St. Louis, MO 63110
JOHN E. GERICH
Endocrine Research Unit, Mayo Clinic, Rochester, MN 55905

REFERENCES AND NOTES

1. E. Mezey *et al.*, *Science* **226**, 1085 (1984).
2. G. B. Boli *et al.*, *N. Engl. J. Med.* **311**, 1214 (1984).
3. R. A. Rizza, P. E. Cryer, J. E. Gerich, *J. Clin. Invest.* **64**, 62 (1979); D. A. Popp, S. D. Shah, P. E. Cryer, *ibid.* **69**, 315 (1982); D. A. Popp, T. F. Tse, S. D. Shah, W. E. Clutter, P. E. Cryer, *Diabetes Care* **7**, 243 (1984).
4. T. F. Tse, W. E. Clutter, S. D. Shah, P. E. Cryer, *J. Clin. Invest.* **72**, 278 (1983).
5. S. G. Rosen, W. E. Clutter, M. A. Berk, S. D. Shah, P. E. Cryer, *ibid.* **73**, 405 (1984).
6. G. Bolli *et al.*, *Diabetes* **32**, 134 (1983); N. H. White *et al.*, *N. Engl. J. Med.* **308**, 485 (1983).